Diagnosing Belt Conveyor Idler Faults with STFT and CNN

Miloš Milovančević

Faculty of Mechanical Engineering, University of Niš, A. Medvedeva 14, Serbia.
E-mail: milos.milovancevic@gmail.com

(Received 23 May 2024; accepted 25 July 2024)

Belt conveyors are widely used for transporting bulk commodities, and idlers are essential components prone to frequent failures. The timely and accurate fault diagnosis of idlers is critical for ensuring the safe and efficient operation of belt conveyors. This paper proposes a method for diagnosing idler faults by combining Short-Time Fourier Transform (STFT) and Convolutional Neural Networks (CNN). The STFT is used to convert one-dimensional vibration signals into time-frequency representations, which are then processed by the CNN to classify the operational state of idlers. The proposed method is tested on vibration signals collected under various working conditions, including normal operation, bearing damage, and cylinder skin fracture. The CNN model, trained and validated using MATLAB, achieves high diagnostic accuracy, demonstrating its effectiveness in identifying different fault types. This approach enhances the reliability of belt conveyor systems by enabling prompt detection and maintenance of idlers.

1. INTRODUCTION

Belt conveyors are widely used for transporting bulk commodities. Idlers, as essential and prevalent components on belt conveyors, are prone to frequent failures. Timely diagnosis of idler problems is crucial for the safe operation of belt conveyors. At present, neither human nor robotic examinations can precisely identify idler faults immediately, which can lead to significant damage and potential safety hazards such as fires. Time-frequency analysis approaches like wavelet analysis, empirical mode decomposition, and local mean decomposition are commonly used in signal processing and feature extraction. However, these techniques have limitations in breaking down the initial signal. Short-Time Fourier Transform (STFT), in contrast, can acquire both time-domain and frequency-domain details simultaneously, providing a more accurate representation of the roller's fault status information. Several studies have demonstrated the effectiveness of combining STFT with advanced models for fault diagnosis. For instance, Fu Zhongguang et al. used STFT with Mobile-VIT network models for fault diagnosis in rotating machinery, while Long Jun et al. applied STFT in conjunction with Hilbert Huang transform for wind turbine generator bearings. Deep CNNs, initially used in image processing and voice recognition, have shown promising results in mechanical fault detection. Liu Huibin et al. utilized CNNs for analyzing bearing faults, and Janssens et al. employed FFT preprocessed signals with CNN for a vibration signal feature extraction and diagnosis. In this paper, we propose a method that combines STFT with CNN to diagnose idler faults. The STFT-derived time-frequency maps are fed into a CNN model to detect normal operation, bearing damage, and cylinder skin damage in idlers. The goal of this method is to enhance the reliability and efficiency of belt conveyor systems by enabling timely maintenance. Belt conveyors are widely used for transporting bulk commodities. Idlers are the essential and prevalent components on belt conveyors. Idler failures often happen during the operation of belt conveyors. Delaying the diagnosis of idler problems will severely limit the safe functioning of the idlers. At present, neither human nor robotic examinations can precisely identify idler faults immediately, resulting in harm to the belt conveyor and may potentially create a fire.[1,2] Wavelet analysis, empirical mode decomposition, and local mean decomposition are commonly used in signal processing and feature extraction. However, these techniques can only break down the initial signal, whereas only STFT can acquire both the time-domain and frequency-domain details of the roller vibration signal simultaneously, allowing for a more accurate representation of the roller's fault status information. Fu Zhongguang and colleagues utilized STFT and Mobile-VIT network models to extract features from time-frequency maps for fault diagnosis of rotating machinery. Long Jun, Wu Jinqiang, Wang Chonghe, and others extracted fault signals from a wind turbine generator bearing using Hilbert Huang transform analysis and short time Fourier transform analysis. After a comparative examination, it was determined that the STFT analysis approach offers excellent time-frequency resolution. Li Heng and colleagues analysed vibration data from rolling bearings using STFT and detected kinds of bearing problems using CNN fault diagnostic models. We suggested a potent defect diagnostic approach through ongoing enhancement.[3]

Deep convolutional networks are often used in image processing and voice recognition. Recently, several academics domestically and internationally have used convolutional network technology to detect mechanical flaws. Liu Huibin et al.[4] used convolutional neural networks and manual extraction to analyze bearing faults from complex sources, demonstrating the effective fault diagnosis capability of CNNs. Janssens et al.[5] preprocessed bearing signals with FFT and utilized CNN to extract and diagnose vibration signal features for bearing fault detection. Dong Xinmin et al.[6] introduced a fault diagnosis model for rotating machinery based on vector spectrum and L-M neural network, comparing the results with single channel data diagnosis and achieving positive outcomes.

This article suggests a technique for identifying the operational condition of idlers by combining STFT with CNN. The STFT-derived time-frequency map is fed into the CNN model to detect normal operation, bearing damage, and cylinder skin damage in idlers.

2. METHOD FOR COLLECTING VIBRATION SIGNALS OF IDLERS

2.1. Vibration Signal Detection Method

Idlers play a significant function in belt conveyors and are one of the important components for proper operation of conveyor belts.[7] Under normal conditions, idlers may decrease friction between the conveyor belt and the metal structure, therefore avoiding wear and damage. Once the supporting roller malfunctions, it will increase the friction between the conveyor belt and the supporting roller frame, causing irregular contact between the fault point and the bearing, generating abnormal vibration pulses, which are significantly different from the vibration pulses during normal operation of the supporting roller. Therefore, it may be established that the supporting roller has failed. In order to assure the accuracy and efficiency of roller defect detection, a distributed optical fiber detection approach is developed. The optical fiber is placed within the channel steel on both sides of the belt conveyor via ties to detect the operational condition of the roller.

When the roller on the belt conveyor fails, an aberrant signal will be presented, and the laser will create a sequence of continuous coherent light. The abnormal signal is converted into an optical pulse by an acousto-optic modulator (AOM). An optical fiber amplifier (EDFA) then amplifies and processes this signal, making it more comprehensive. The photoelectric pulses are then progressively linked to the optical cable via an isolator and a ringer. When the optical pulse signal flows through the optical fiber. Rayleigh scattering is formed, and the backscattered Rayleigh light returns to the ringer following the original route of the optical fiber.[8] The gathered signal is denoised to verify its correctness of the aberrant signal. The optical pulse signal is filtered and transformed to an electrical signal using a photodetector. Real-time detection is then performed utilizing a data acquisition card. Many duties are performed on the computer, including display, processing, and analysis, to enhance the accuracy and comprehensiveness of fault signal processing.

The motivation behind this study is to address the limitations of existing methods in diagnosing idler faults promptly and accurately. The proposed approach leverages the strengths of STFT in capturing detailed time-frequency information and the capability of CNNs in feature extraction and classification.

More references are integrated to support the background and existing methods:

- A dual-attention feature fusion network for imbalanced fault diagnosis with two-stream hybrid generated data;[9]
- Few-shot Learning for Fault Diagnosis with a Dual Graph Neural Network. IEEE Transactions on Industrial Informatics;[10]
- Online Fault Diagnosis Method based on Transfer Convolutional Neural Networks. IEEE Transactions on Instrumentation and Measurement.[11]

While STFT and CNN are existing methods, our approach highlights specific innovations:

- Enhanced preprocessing of vibration signals using STFT to create more accurate time-frequency representations; and,

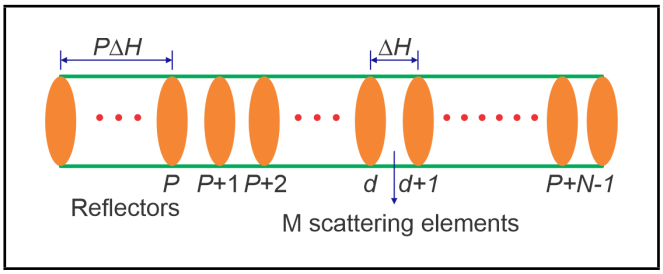

Figure 1. φ-OTDR principle discrete model.

- Integration of a robust CNN architecture optimized for fault diagnosis in idlers, with improved parameter tuning and validation.

The dataset used in this study is thoroughly described. Vibration signals were collected under various working conditions, including normal operation, bearing damage, and cylinder skin fracture. Ablation experiments were conducted to validate the improved parts of the proposed method.

The vibration signals were collected using a distributed optical fiber detection approach. The dataset includes signals from normal operation, bearing damage, and cylinder skin fracture conditions. Ablation experiments were conducted to isolate and test the impact of specific components of the proposed method. The results highlight the improvements achieved by the enhanced STFT preprocessing and the CNN model configuration.

2.2. Base on Vibration Signal Conversion Using φ-OTDR Technology

Backward Rayleigh scattering(φ-OTDR) phenomenon is a refinement of the traditional Rayleigh scattering principle, utilizing the φ-OTDR discrete model can intuitively describe the above process, as shown in Fig. 3. Which can help readers understand more clearly and intuitively that the working principle of φ-OTDR is to treat the distributed optical fibers at each roller in the belt conveyor roller group as a reflector whose reflectivity is related to the incident light wave. The H-length optical fibers arranged on the belt conveyor frame are composed of P-segments, with each segment having a length of $\Delta H = H/P$. Distributed optical fiber φ-OTDR phenomenon is due to the fact that a portion of the incident light is returned to the fiber when it is transmitted to a small segment in the fiber. After being reflected by the P-segment, the reflectivity of the above-mentioned mirrors is lower, and they are all weaker mirrors.

As shown in Fig. 1, the d-th reflector in the figure is considered as the center of discretization in the ΔH fiber region. This small segment of fiber ΔH contains N discretization centers. Therefore, multiple backward Rayleigh scattered light at the H_n position on the distributed fiber will interfere, and the superposition of light fields can be written as follows:

$$\vec{E}_{RB}(H_n) = E_0 e^{-\alpha(n-1)\Delta H} \sum_{i=1}^{N} a_i^n e^{j\varphi_i^n}. \quad (1)$$

In the above equation, E_0 is the electric field of the incident light, α is the attenuation coefficient of the optical fiber, a_i^n and φ_i^n is the amplitude and phase of the i-th discretization center in Part n, respectively.

Due to the birefringence phenomenon generated by optical fibers during transmission, the polarization state within a unit

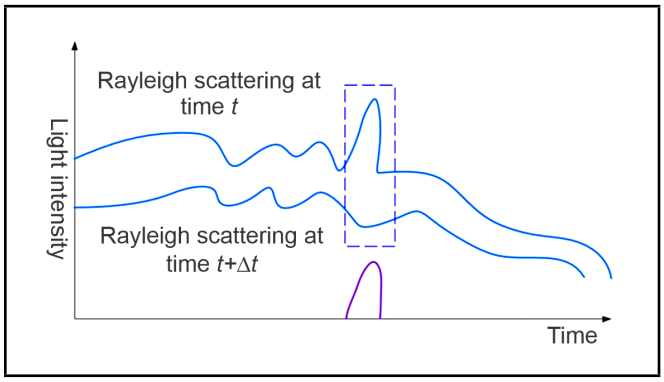

Figure 2. Time domain curve of Rayleigh scattering before and after fault.

length of ΔH gradually changes along the distributed fiber, resulting in an elliptical shape of the detected backward Rayleigh scattering light signal. As shown in Fig. 2, when there is little external environmental interference, there will be significant amplitude changes before and after the vibration at the fault location. However, the amplitude before and after the vibration at the normal working position remains almost unchanged. Therefore, the fault location can be located by subtracting the Rayleigh scattering amplitude curve before and after the vibration.

3. METHOD FOR PROCESSING VIBRATION SIGNALS OF IDLERS

Signal processing is crucial for detecting faults in the intermediate segment of the belt conveyor idler. The accuracy of fault detection depends on the quality of signal processing. This paper utilizes STFT and CNN to analyze vibration signals from the idler under various working conditions, enhancing the accuracy of detecting the idler's operational state and providing a theoretical basis for fault detection in the intermediate section of the belt conveyor idler.

3.1. STFT

STFT has been widely used in time-frequency analysis of time-varying and non-stationary signals. It is a method of converting one-dimensional fault vibration signals into two-dimensional matrices that can be used for CNN processing. It is a collection of time-domain and frequency-domain features. STFT is the process of taking a certain length of a time-domain signal as a window function, and further performing FFT on the intercepted time-domain signal to obtain the spectrum graph over a time period t. By sliding the window function over the detection time period, the set of each spectrum segment can be obtained. Therefore, STFT is a two-dimensional function of time and frequency,[12] and the basic calculation formula is as follows:

$$STFS_f(t,f) = \int_{-\infty}^{\infty} h(t)p(t-\beta)e^{-j\omega t}dt. \tag{2}$$

In the above equation, $h(t)$ is the time-domain signal; $P(t-\beta)$ in order to β the time window centered on STFT is the multiplication of the vibration signal $h(t)$ by a β Window function $p(t-\beta)$. The area of the window function in the FFT performed is a certain amount. In order to improve the time-domain and frequency-domain resolution, this study selects the Hamming window function.

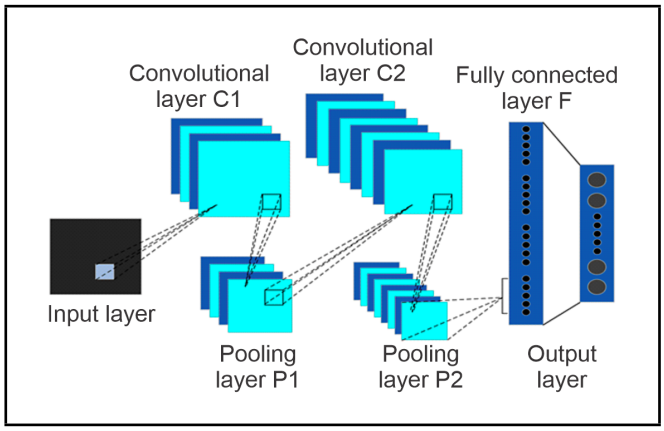

Figure 3. Convolutional neural network structure.

3.2. CNN

CNN is a feedforward neural network widely used in image and speech classification and recognition, which can effectively handle fault diagnosis and achieve deep learning under big data.[13] Since LeNet-5 was proposed by Lecun et al.,[14] the structure of CNNs can be designed according to requirements, mainly consisting of convolutional layers, pooling layers, and fully connected layers, as shown in Fig. 3.

CNNs process vibration signals by taking the time-frequency spectrum obtained from the STFT as the input signal and outputting the type of roller fault as the CNN model. The CNN diagnostic model divides the process of signal processing into forward propagation and backward propagation.[15]

3.2.1. Forward propagation

The forward propagation process of CNNs includes convolutional layers, pooling layers, and fully connected layers.[16]

Convolutional Layer: The convolutional layers extract features from input signals by applying filters. Each filter slides on the input and obtains corresponding feature maps. By stacking multiple convolutional layers, the features in the CNN model become more comprehensive. Finally, the convolutional layer outputs a set of feature maps that represent the responses of different features. These feature maps can be transmitted to the pooling layer for further processing. The mathematical expression for the convolution process is as follows:

$$W_j^p = f\left(\sum_{i\in H_j} W_i^{p-i}\cdot q_{ij}^p + k_j^p\right). \tag{3}$$

In the above equation, W_j^p is the j-th element of the p-th layer, H_j is the j-th convolutional region of the $p-1$ layer feature map, W_i^{p-1} is the element in it, q_{ij}^p is the weight matrix corresponding to the convolutional kernel, k_j^p is the bias term, $f(\cdot)$ is the activation function, and by using the ReLU function, the specific expression is:

$$f(x) = \max(0, \log(1+e^x))). \tag{4}$$

Pooling Layer: Pooling layer is a commonly used layer in CNN models, which can reduce the size and number of feature maps. It divides the input feature map into nonoverlapping regions $n \times n$, and performs aggregation operations on

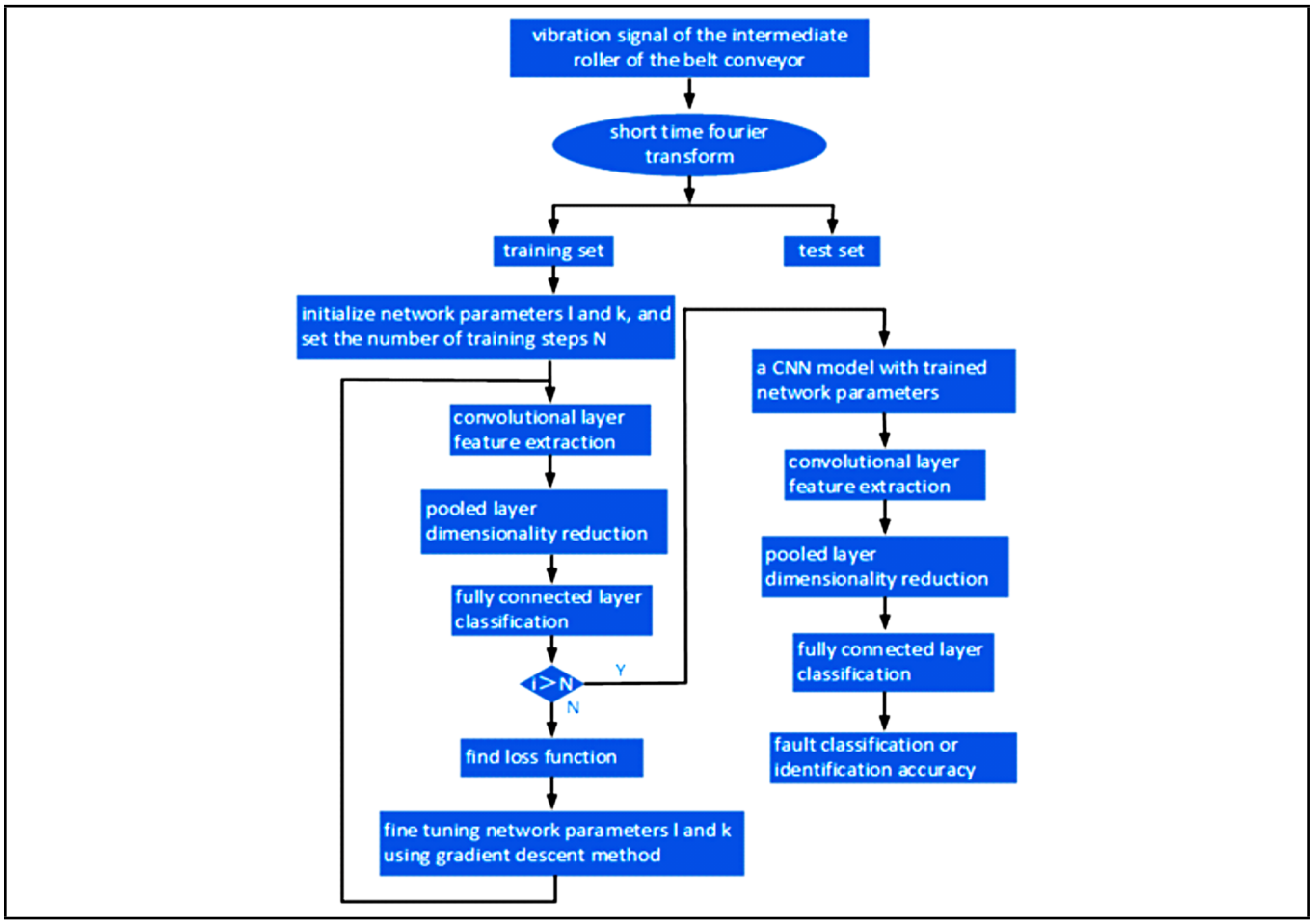

Figure 4. Fault diagnosis flowchart of convolutional neural network.

each region, such as taking the maximum, average, and random values, to reduce the output image by n times. This can reduce the size of the feature map while retaining key information. The pooling layer improves computational efficiency by reducing dimensions and enhances the model's robustness to translation and scaling changes. Finally, the pooling layer outputs feature maps that have undergone aggregation operations, with smaller sizes and richer representation capabilities for use by subsequent layers.

Fully Connected Layer: The input time-frequency image is processed through convolutional and pooling layers, and then reaches the fully connected layer for feature recognition. The fully connected layer expands all input feature spectra into one-dimensional feature vectors, and performs weighted summation and activation function processing on them:[17]

$$y^m = f(l^m x^{m-1} + k^m). \tag{5}$$

In the above equation, m is the serial number of the network layer, y^m is the output of the fully connected layer, x^{m-1} is the expanded one-dimensional feature vector, l^m is the weight coefficient, and k^m is the bias term. $f(\cdot)$ is the activate function, the Softmax function is usually used, which is an activation function suitable for classification tasks.[18,19]

3.2.2. Back Propagation

For specific diagnostic recognition, the training goal of the CNN model is to minimize the loss function of the network, so the loss function determines the diagnostic accuracy of the CNN model. In this study, cross entropy is chosen as the loss function, and the specific expression is as follows:

$$E = -\frac{1}{n}\sum_{m=1}^{n}\left[y_m \ln t_m + (1-y_m)\ln(1-t_m)\right]. \tag{6}$$

In the above equation, n is the number of samples for roller failure, t is the predicted value, and y is the true value. During the training process, the first order partial derivative of the above equation is applied to gradually update the parameters of the CNN

$$l' = l - \eta\frac{\partial E}{\partial l}; \tag{7}$$

$$k' = k - \eta\frac{\partial E}{\partial k}. \tag{8}$$

In the above equations, l' and k' are the updated weights and biases, l and k are the existing weights and biases, η is learn rate parameters for neural networks. If η excessive values can lead to local optima, if the value is too small, it will cause too long of a training time.

3.3. Diagnosis Process for Intermediate Section Roller Faults

The roller defect diagnosis approach utilizes STFT and CNN models to combine signal preprocessing, feature extraction, and classification. Figure 4 illustrates the precise technique. The vibration signals of the roller acquired under various operating situations are processed using STFT. The resulting spectrum is fed into a CNN model for training and testing.

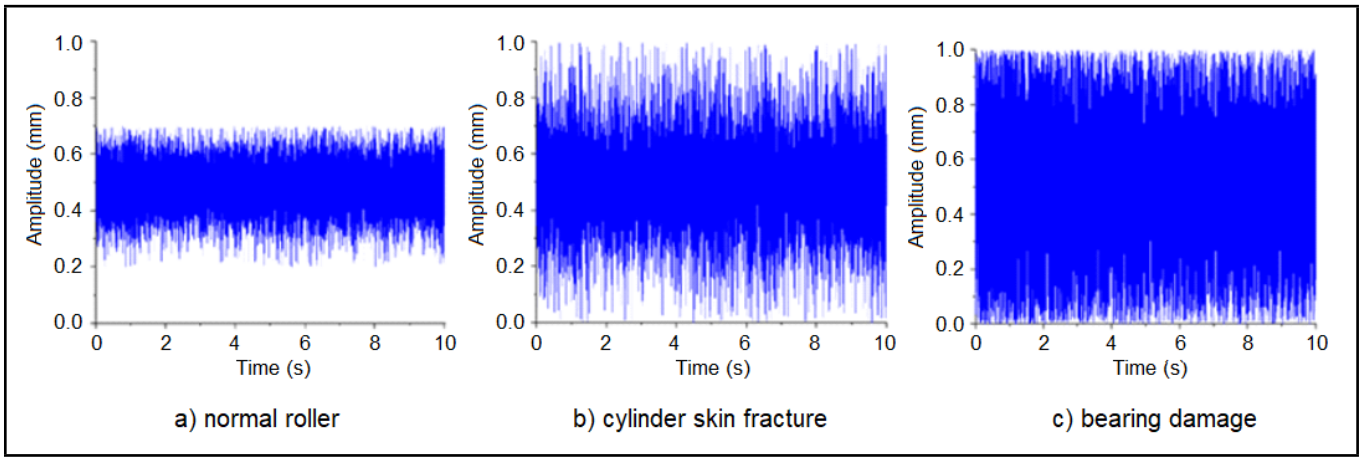

Figure 5. Amplitude time correspondence curve of idler under different working conditions.

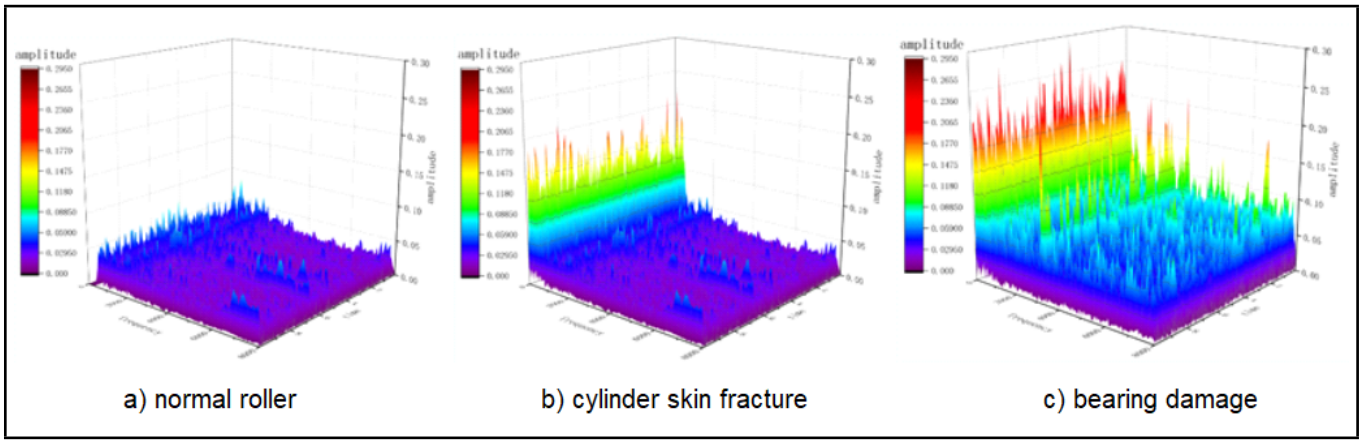

Figure 6. Time frequency diagram of roller under different working conditions.

The training set's spectrum is first fed into the CNN model, and the network parameters of the CNN model are iteratively updated. Once the CNN model achieves a certain level of accuracy via continual refinement, it is used on the testing set to get fault diagnostic findings for the roller.

4. SIGNAL PROCESSING

This section pertains to the real working conditions of the intermediate section idler of a certain mining belt conveyor. It is recommended to extract the vibration signals from both normal and faulty operation situations of the intermediate part of the belt conveyor. Subsequently, STFT processing is used for these retrieved signals to provide a response spectrum. The frequency spectrum is used as input for the CNN model to determine the operational condition of the idler.

4.1. Vibration Signal Based on STFT

Standardize the operational data of the roller collected from scattered fibre optic sensors. Figure 5 displays the data for the roller under normal operation, bearing damage, and cylinder skin fracture situations. The roller's amplitude is minimal under normal conditions but increases significantly with bearing deterioration and cylinder skin fracture, showing more pronounced shifts within the $[0, 1]$ range. Further analysis of the collected vibration signal is required.

Conduct STFT on the normalized data acquired. Figure 6 displays the time-frequency distribution of the STFT under various operating circumstances of the supporting roller. The supporting roller operates under varying circumstances, leading to fluctuations in time-frequency information. When analyzing the time-frequency signals of the belt conveyor supporting roller under normal operation, bearing damage, and cylinder skin fracture conditions, it is evident that the vibration signal frequency of the supporting roller is minimal during normal operation, with an amplitude below 0.059 mm. If the roller malfunctions because of the cylinder skin breaking, the vibration signal frequency distribution of the problematic roller during operation ranges from 0 to 500 Hz. At 100 Hz, the frequency energy peaks with a maximum amplitude of around 0.18 mm. If the roller fails because of a bearing failure, the vibration signal frequency appears dispersed, with the highest frequency usually centred around 100 Hz, and the greatest amplitude reaching around 0.27 mm.

4.2. Fault Identification Based on Convolutional Neural Networks

The experimental results demonstrate the high accuracy of the proposed method in diagnosing idler faults. The CNN model trained with STFT-processed signals achieved a diagnostic accuracy of 99.6% with MATLAB. The robustness of the model was further validated through tests at different belt speeds, confirming its effectiveness across various working conditions. The parameter configurations of the convolutional layer, pooling layer, and fully connected layer are crucial for the accuracy of CNN diagnostic models. In the following section, we develop a CNN model in MATLAB software for de-

Table 1. Structural parameters of CNNs.

Model parameter	Input layer	Pooling layer	Convolutional layer	Pooling layer	Convolutional layer	Pooling layer	Fully connected layer	Output layer
Number of feature maps	1	1	32	32	64	64	1	1
Feature map size	64×64	32×32	32×32	16×16	16×16	8×8	2048	1

fect detection of the middle section roller of a belt conveyor, using the parameters specified in Table 1.

The STFT-processed vibration signal spectrum serves as the input for an 8-layer CNN for processing. This article's CNN model directly invokes the image datastore function provided by MATLAB programme. The dataset is imported into the function, and then the training and testing sets for the roller's operating conditions are separated. There are 1000 samples in all, with 750 in the training set and the remaining in the testing set. The training samples are randomly selected to acquire the training data. The CNN model in the training network goes through four rounds of iteration with a validation frequency of 30 iterations. Training stops when the maximum number of rounds is reached to calculate the accuracy and loss values for the training and validation sets, as seen in Figs. 7 and 8 below.

The dataset in this article contains three distinct kinds of roller operating circumstances, each consisting of 1000 samples, totaling 3000 samples. A training set consisting of 2250 samples and a testing set of 750 samples were established, and the training procedure included "packet capturing". Following each training session, the outcomes were implemented on the test dataset. A comparison was made between the diagnosed roller operating circumstances and the actual operating conditions to determine the accuracy and loss values of the CNN model. Figure 7 illustrates a significant improvement in accuracy for both the training and validation sets over the first two rounds of iterations, surpassing 95% accuracy. The training set converged after 20 rounds, but the validation set stabilized after 30 iterations. With each cycle, the training and validation sets steadily approached their peak accuracy. Figure 8 shows that the loss values for both the training and validation sets were about 2.5 at the start of the cycle. After the first iteration, the training set's loss values dropped to around 0.2, while the validation set's loss values declined to about 0.8. After 30 iterations of the CNN model, the loss values for the validation set reduced to around 0.1. As the iterations grew, the loss values of the training and validation sets steadily approached the minimum. The CNN model described in this paper achieves a recognition accuracy of 99.6% for three kinds of roller operation states, enhancing the efficiency of roller operation conditions, particularly in roller fault diagnostics.

4.3. Robustness Verification

The CNN model's accuracy in recognizing the roller's operating conditions is evaluated using the frequency spectrum of vibration signals from the central region of the belt conveyor roller under various working situations. The acquired data pertains to the belt conveyor operating speed of 4 m/s. In the new dataset, belt speeds of 3 m/s and 5 m/s are included to test the detection method's universality in real working conditions and task demands. At belt speeds of 3 m/s and 5 m/s, there are 1000 samples for each condition, totaling 6000 samples. These samples are divided into 10 groups. The remaining parameter values are identical to those of 4 m/s. Figure 9 displays a comparison of CNN accuracy in detecting the operational condition of the roller at three different belt speeds.

The CNN diagnostic model derived from the background of a belt conveyor at a speed of 4 m/s is specifically effective in accurately detecting the operating status of the idlers at that speed, but is not suitable for recognizing the idlers' operating status at different belt speeds. The CNN diagnostic model being examined lacks universality. It is essential to create a comprehensive dataset that contains the idlers' operating status characteristics at various belt speeds of the conveyor belt. This data should be promptly fed into the CNN model to expand the dataset, enabling the model to recognize idlers' operating status in a wider range of working conditions.

The vibration signals were collected over a period of time and the CNN model was enhanced to assess the operational condition of the idlers at belt speeds of 3 m/s, 4 m/s, and 5 m/s. 9000 samples were designated as validation datasets, and network parameters were trained and used on the test set. Figure 10 demonstrates the updated CNN model's precision in recognizing the idlers' functioning state in various working situations.

The CNN model's training and testing sets have been enhanced by collecting vibration signals at various belt speeds and idler working circumstances, as shown in Fig. 10. The model efficiently detects the idlers' working conditions in belt conveyors at various belt speeds, demonstrating that the CNN model is a dataset-driven recognition approach. Greater data collection leads to more comprehensive identification patterns and, thus, increased diagnosis accuracy. This research solely examined the impact of typical belt speeds of belt conveyors on the working conditions of idlers in the CNN model, owing to financial constraints and location limits. Future research will analyze how elements like average transportation volume and noise from belt conveyors affect the working conditions of idlers.

5. CONCLUSIONS

This study presents a novel approach for diagnosing belt conveyor idler faults by combining STFT and CNN. The method effectively processed vibration signals and accurately classified the operational states of idlers, contributing to the reliability and efficiency of belt conveyor systems. Future research will focus on expanding the dataset and further improving the model's robustness. The paper suggests a technique for assessing the operational condition of the intermediate section idler of a belt conveyor using STFT and CNN. This involved: 1) preprocessing the vibration signals from the middle section of the belt conveyor's idler operation; 2) extracting and classifying numerous features including normal idler operation, damaged idler bearings, and broken idler cylinder skin to achieve precise idler fault diagnosis; and, 3) using distributed fibre optic vibration signals, the vibration signal characteristics of the intermediate section roller of a specific mining belt conveyor. All of these were collected and examined under various operating conditions. These characteristics were then analyzed using STFT to determine the frequency spectrum of the roller under different working conditions. A CNN model was constructed using MATLAB software, and the network model parameters were adjusted based on real on-site circumstances.

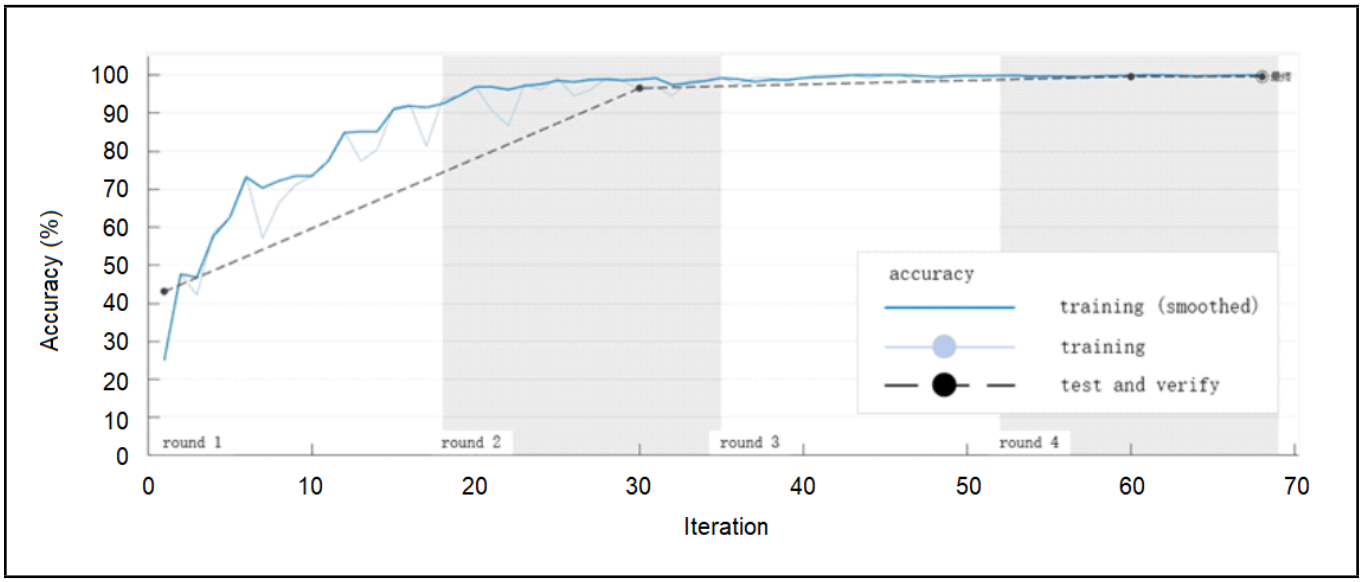

Figure 7. Accuracy test results for training and validation sets.

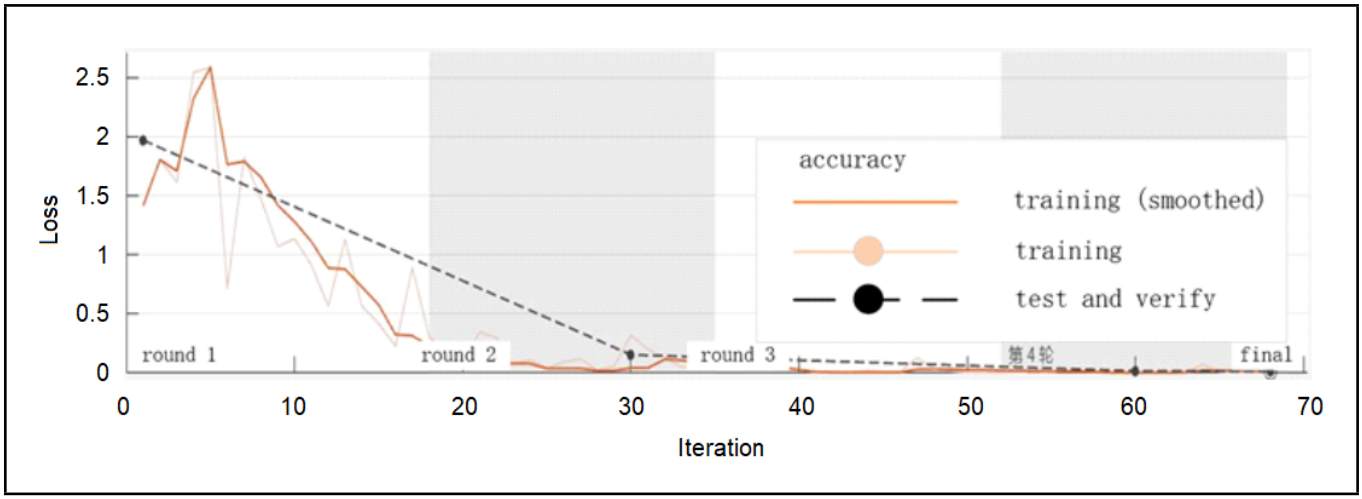

Figure 8. Test results of loss values for training and validation sets.

Next, the acquired spectrum was fed into the CNN model to determine the operational condition of the rollers. Optimization of the CNN model network parameters was utilized to properly identify the operational condition of the rollers. This study reached the following conclusions:

- Analyzing the roller's vibration signal using STFT may provide the spectrum, allowing for an accurate assessment of the roller's operational status. By feeding the spectrum into the CNN model and iteratively optimizing the network parameters, improved recognition outcomes may be obtained.

- The CNN diagnostic model in this article enhances the accuracy of detecting the roller's operating state in the MATLAB programme as the number of repetitions rose. During the second iteration, the CNN model achieved its highest accuracy, which peaked around the maximum value. By the fourth iteration, the diagnostic accuracy reached a maximum of 99.6%. During on-site verification, the CNN diagnostic model had an accuracy of 96.5% and an error rate of 3.1%. Thus, the CNN model maintained a high level of accuracy.

REFERENCES

[1] Qi, Q., Wang, H.,Dong, Z., et al. Numerical simulation study on the fire propagation law of belt conveyor tunnels in mines (in Chinese), *Chinese Journal of Safety Science*, **26** (10), 36–41, (2016).

[2] Li, C., Li, C., Liang, M., et al. Analysis of accidents and protective measures for coal mine belt conveyors (in Chinese), *Chinese Journal of Safety Science*, 2006 (03), 140–144, 148, (2006).

[3] Jin, J., Xu, Z., Li, C., et al. Fault diagnosis of rolling bearings based on deep learning and chaotic feature fusion (in Chinese), *Control Theory and Application*, **39** (01), 109–116, (2022).

[4] Liu, H., Li, S., Zhang, A., et al. Research on bearing multi fault diagnosis based on deep convolutional neural networks (in Chinese), *Combined Machine Tool and Automation Processing Technology*, **2020** (05), 12–16, (2020).

[5] Janssens, O., Slavkovikj, V., Vervisch, B., et al. Convolutional neural network based fault detection for rotating

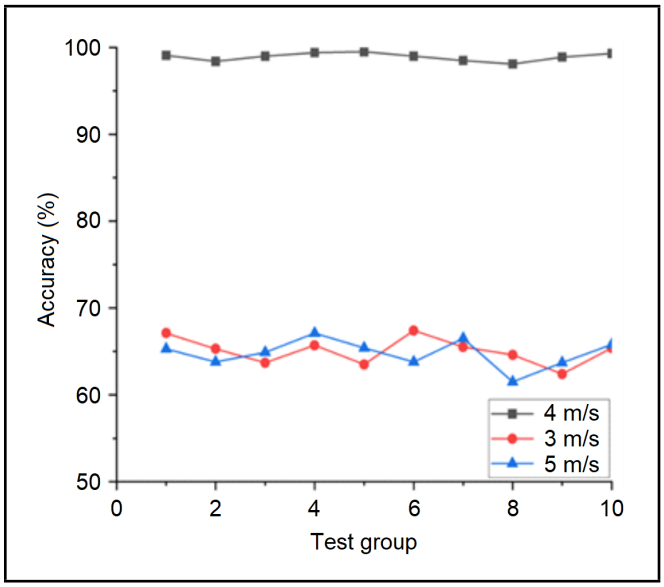

Figure 9. Comparison of CNN model recognition results under different belt speeds.

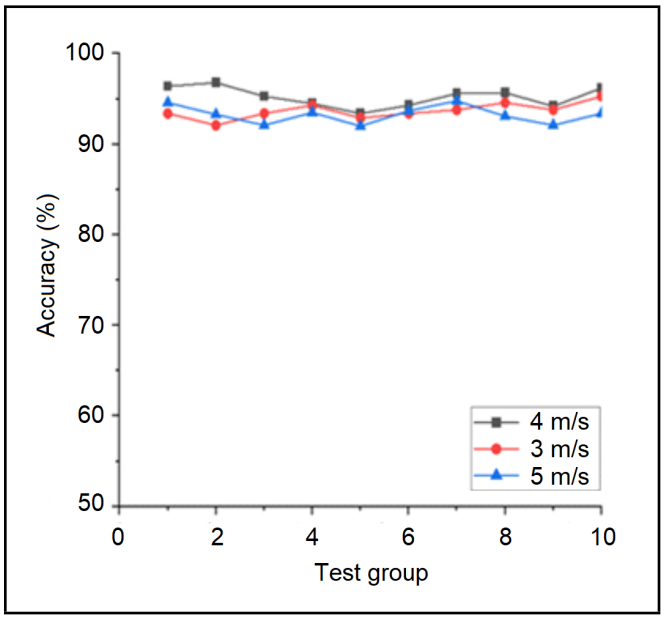

Figure 10. Comparison of CNN model recognition results under different belt speeds under big data.

machinery, *Journal of Sound and Vibration*, **377**, 331–345, (2016). https://doi.org/10.1016/j.jsv.2016.05.027

[6] Dong, X., Han, J., Shi, L., et al. Research on fault diagnosis of rotating machinery based on vector spectrum and L-M neural network (in Chinese), *Steam Turbine Technology*, **51** (05), 372–375, (2009).

[7] Xie, H., Bao, J., Ge, S., et al. Experimental study on the rotating resistance characteristics of belt conveyor carrying idlers (in Chinese), *Journal of Coal Industry*, **44** (S2), 731–736, (2019).

[8] Li, X., Liang, H., Xu, W., et al.: Comparison of performance of commonly used distributed fiber optic sensors (in Chinese), *Optical Communication Technology*, **2007** (05), 14–18, (2007).

[9] Wang, C., Wang, H., and Liu, M. A dual-attention feature fusion network for imbalanced fault diagnosis with two-stream hybrid generated data, *Journal of Intelligent Manufacturing*, **35**, 1707–1719, (2024). https://doi.org/10.1007/s10845-023-02131-2

[10] Ramírez-Sanz, J. M., Maestro-Prieto, J.-A., Arnaiz-González, Á., and Bustillo, A. Semi-supervised learning for industrial fault detection and diagnosis: A systemic review, *ISA Transactions*, **143**, 255–270, (2023). https://doi.org/10.1016/j.isatra.2023.09.027

[11] Xu, G., Liu, M., Jiang, Z., Shen, W., and Huang, C. Online fault diagnosis method based on transfer convolutional neural networks, *IEEE Transactions on Instrumentation and Measurement*, **69** (2), 509–520, (2020). https://doi.org/10.1109/TIM.2019.2902003

[12] Xu, J. *Research on Bearing Fault Diagnosis Method Based on Double Tree Complex Wavelet and Width Learning* (in Chinese), Inner Mongolia University of Science and Technology, (2020).

[13] Krizhevsky, A., Sutskeve, R. I., and Hinton, G. E. Image N classification with deep convolutional neural networks, *International Conference on Neural Information Processing Systems*, Curran Associates Inc., 1097–1105, (2012).

[14] LeCun, Y., Bose, R. B., Denker, J. S., et al. Back propagation applied to hand written zip code recognition, *Neural Computation*, **1** (4), 541–551, (1989). https://doi.org/10.1162/neco.1989.1.4.541

[15] Yuan, M. *Research on Typical Target Detection Algorithms in Remote Sensing Images Based on Deep Learning* (in Chinese), Strategic Support Force Information Engineering University, (2020).

[16] Chu, Y. *Research on fine-grained image classification based on deep residual networks* (in Chinese), Nanjing University of Posts and Telecommunications, (2020).

[17] Li, D., Niu, J., Liang, S., et al. Intelligent diagnosis of wheel faults based on multi-scale time-frequency maps and convolutional neural networks, *Journal of Railway Science and Engineering* (in Chinese), **20** (03), 1032–1043, (2023).

[18] Ryba, T., Rucki, M., Siemiatkowski, Z., Bzinkowski, D., and Solecki, M. Design and calibration of the system supervising belt tension and wear in an industrial feeder, *Facta Universitatis, Series: Mechanical Engineering*, **20** (1), 167–176, (2022). https://doi.org/10.22190/FUME201004026R

[19] Mobki, H., Sedighi, M., Azizi, A., and Eskandari, M. Designing an efficient observer for the non-linear Lipschitz system to troubleshoot and detect secondary faults considering linearizing the dynamic error, *Facta Universitatis, Series: Mechanical Engineering*, **20** (3), 677–691, (2022). https://doi.org/10.22190/FUME220528043M